ORIGINAL ARTICLE

NUMERICAL MODELING ON AN UNSTEADY LAMINAR BOUNDARY LAYER FLOW USING NANO FLUID WITH VISCOUS DISSIPATION EFFECT AND HEAT SOURCE THROUGH A STRETCHING SHEET

| Shahmin Akter [1] | M Enamul Karim [1] |and | Noor Alam [2*] |

[1.] Comilla University | Department of Mathematics | Cumilla-3506 | Bangladesh |
[2.] Primeasia University | Department of Basic Science | Dhaka-1213 | Bangladesh |

| Received September 09, 2020 | | Accepted October 8, 2020 | | Published October 23, 2020 | | ID Article| Noor–Ref2-ajira011020 |

ABSTRACT

Background: The nanofluid in view of the fabulous thermal conductivity enhancement have been recognized useful in several industrial and engineering applications. **Methods**: The unsteady laminar boundary layer flow using Nano fluid with viscous dissipation effect and heat source along a stretching sheet has been investigated numerically. To obtain non - similar equations, continuity, momentum, energy, and concentration equations have been non-dimensionalized by usual transformation. **Results**: The non-similar solutions are considered here which depend on the Prandtl number P_r , Eckert number E_c , Lewis number L_e , Brownian motion parameter N_b, thermophoresis parameter N_t and Grashof number G_r. The obtained equations have been solved by an explicit finite difference method with stability and convergence analysis. This method is a powerful technique for obtaining the approximate solution of the boundary value problems. The velocity, temperature, and concentration profiles are shown in graphically for different time steps and for the different values of the parameters.
Keywords: *Nanofluid, Stretching surface, Viscous dissipation.*

1. INTRODUCTION

The nanofluid in view of the fabulous thermal conductivity enhancement have been recognized useful in several industrial and engineering applications. Working fluids have great demands placed upon them in terms of increasing or decreasing energy release to systems, and their influences depend on thermal conductivity, heat capacity and other physical properties in modern thermal and manufacturing processes. A low thermal conductivity is one of the most remarkable parameters that can limit the heat transfer performance. In addition, the classical heat transfer fluids such as ethylene glycol, water and engine oil have limited heat transfer capabilities due to their low thermal conductivity and thus cannot congregate with modern cooling requirements. On the other hand thermal conductivity of metals is extremely higher in comparison to the conventional heat transfer fluids. Suspending the ultrafine solid metallic particles in technological fluids causes an increase in the thermal conductivity. This is one of the most modern and appropriate methods for increasing the coeffcient of heat transfer.

The flow over a stretching sheet is an important problem in many engineering processes with applications in industries such as an extrusion melt spinning, the hot rolling and colling of a large metallic plate in a bath.

Magnetohydrodynamics (MHD) boundary layer flow of nanofluid and heat transfer over a linearly stretched surface have received a lot of attention in the field of several industrial, scientific, and engineering applications in recent years. Nano fluids have many applications in the industries since materials of nanometer size have unique chemical and physical properties. With regard to the sundry applications of Nano fluids, the cooling applications of Nano fluids include silicon mirror cooling, electronics cooling, vehicle cooling, transformer cooling, etc. This study is more important in industries such as hot rolling, melt spinning. Extrusion, glass fiber production, wire drawing, and manufacture of plastic and rubber sheets, polymer sheet and filaments, etc.

Sakiadis (2017) was the first author to analyze the boundary layer flow on a continuous surface [1]. Crane ()obtained an exact solution of the boundary-layer flow of the Newtonian fluid caused by the stretching of an elastic sheet moving in its own plane linearly [2]. Gorla et al., (1970, 1987) solved the new similar problem of free convective heat transfer from a vertical plate embedded in a saturated porous medium with an arbitrarily varying surface temperature [3.4]. Cheng and Minkowycz (1977) also studied free convection from a vertical flat plate with applications to heat transfer from a dick [5].

Dissipation is the process of converting mechanical energy of downward-flowing water into thermal and acoustical energy. Various devices are designed in streambeds to reduce the kinetic energy of flowing waters, reducing their erosive potential on banks and river bottoms. Vajravelu and Hadjinicalaou (1993) analyzed the heat transfer characteristics over

*Corresponding author Author: | Shahmin Akter | & Copyright Author © 2020:| Noor Alam [1] |. All Rights Reserved. All articles published in *American Journal of Innovative Research and Applied Sciences* are the property of Atlantic Center Research Sciences, and is protected by copyright laws CC-BY. See:http://creativecommons.org/licenses/by-

a stretching surface with viscous dissipation in the presence of internal heat generation or absorption [6]. Takhar et al., (2002) studied the radiation effects on the MHD free convection flow of a gas past a semi-infinite vertical plate [7]. Ghaly considered the thermal radiation effect on a steady flow, whereas Rapits and Massalas (2002) and El-Aziz (1998) analyzed the unsteady case [8, 9, 10]. Sattar and Alam (1994) presented unsteady free convection and mass transfer flow of a viscous, incompressible, and electrically conducting fluid past a moving infinite vertical porous plate with thermal diffusion effect [11]. Na and Pop (1996) analyzed an unsteady flow due to a stretching sheet [12]. In the case of unsteady boundary-layer flow, Singh et al., (2010) investigated the thermal radiation and magnetic field effects on an unsteady stretching permeable sheet in the presence of free stream velocity [13]. The study of convective instability and heat transfer characteristics of Nano fluids was considered by Kim et al., [14]. Jang and Choi (2009) obtained nanofluid thermal conductivity and the effect of various parameters on it [15].

The natural convective boundary layer flows of a nanofluid past a vertical plate have been described by Kuznetsov and Nield (2009, 2010) [16, 17]. In this model the Brownian motion and thermophoresis are accounted with the simplest possible boundary conditions. They also studied the Cheng-Minkowycz problem for natural convective boundary-layer flow in a porous medium saturated by a nanofluid. Bachok et al., (2010) have shown the steady boundary layer flow of a nanofluid past a moving semi-infinite flat plate in a uniform free stream [18]. It was assumed that the plate is moving in the same or opposite directions to the free stream to define the resulting system of non-linear ordinary differential equations. Khan and Pop (2010, 2011) formulated the problem of laminar boundary-layer flow of a nanofluid past a stretching sheet [19, 20].

They also expressed free convection boundary-layer nanofluid flow past a horizontal flat plate. Hamad and Pop [21] discussed the boundary-layer flow near the stagnation-point flow on a permeable stretching sheet in a porous medium saturated with a nanofluid. Hamad et al., (2011) investigated free convection flow of a nanofluid past a semi-infinite vertical flat plate with the influence of magnetic field [22]. Very recently, Hady et al., (2013) investigated the effects of thermal radiation on the viscous flow of a nanofluid and heat transfer over a non-linearly stretching sheet [23]. However, the aim of the present work is to study the unsteady laminar boundary layer flow using nano fluid with viscous dissipation effect and heat source. An explicit finite difference procedure [24] has been taken to solve the obtained non-similar equations with stability and convergence analysis.

2. MATERIELS AND METHODES

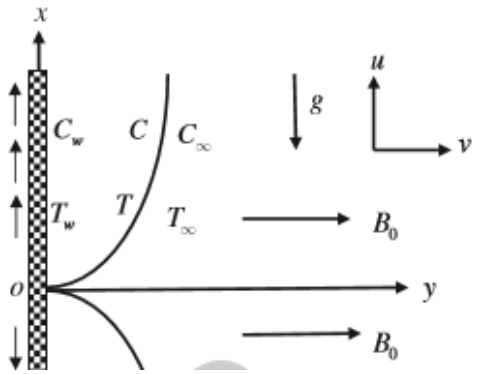

Figure 1: Physical model and coordinate system.

Consider an unsteady two dimensional laminar boundary layer flow of a viscous incompressible Nano fluid along a vertical stretching sheet with dissipation effect. To establish a physical configuration, a two dimensional coordinate system was introduced. The X axis is taken along the stretching sheet in the vertically upward direct

At time $t > 0$, the temperature of the plate raised to $T_W (> T_\infty)$ and the species concentration raised to $C_W (> C_\infty)$, where $T_w$and C_w are the temperature and species concentration at the wall,T_∞ & C_∞ are the temperature and species concentration away from the plate.

Under the boundary layer approximation, the governing equation for the unsteady nanofluid flow expressed as follows:

The continuity equation

$$\frac{\partial u}{\partial x} + \frac{\partial v}{\partial y} = 0 \tag{1}$$

The momentum equation

$$\rho\left(\frac{\partial u}{\partial t} + u\frac{\partial u}{\partial x} + v\frac{\partial u}{\partial y}\right) = \mu\frac{\partial^2 u}{\partial y^2} + g\rho\beta(T - T_\infty) \tag{2}$$

The energy equation

$$\frac{\partial T}{\partial t}+u\frac{\partial T}{\partial x}+v\frac{\partial T}{\partial y}=k_T\frac{\partial^2 T}{\partial y^2}+\frac{\upsilon}{c_p}\left(\frac{\partial u}{\partial y}\right)^2+\tau\left\{D_B\left(\frac{\partial T}{\partial y}.\frac{\partial C}{\partial y}\right)+\frac{D_T}{T_\infty}\left(\frac{\partial T}{\partial y}\right)^2\right\} \quad (3)$$

The concentration equation

$$\frac{\partial C}{\partial t}+u\frac{\partial C}{\partial x}+v\frac{\partial C}{\partial y}=\left[D_B\frac{\partial^2 C}{\partial y^2}+\left(\frac{D_T}{T_\infty}\right)\frac{\partial^2 T}{\partial Y^2}\right] \quad (4)$$

The initial & boundary conditions:

$$t=0,u=Dx,v=0,T=T_\infty,C=C_\infty \ everywhere$$

$$t\geq 0,u=0,v=0,T=T_\infty,C=C_\infty \ at\ x=0$$

$$u=Dx,v=0,T=T_W,C=C_W \ at\ y=0$$

$$u=0,v=0,T\to T_\infty,C\to C_\infty \ at\ y\to\infty$$

Where

u & v are the velocity components in the X and Y direction

υ is the kinematic viscosity

K_T is the thermal conductivity for temperature

C_p is the specific heat at constant pressure

D_B is the Brownian diffusion coefficient

D_T is the thermophoresis diffusion coefficient

g is the acceleration due to gravity

ρ is the density of the fluid

Non dimensional variables:

$$X=\frac{xU_0}{\upsilon},Y=\frac{yU_0}{\upsilon},U=\frac{u}{U_0},V=\frac{v}{U_0},\tau=\frac{tU_0^2}{\upsilon},\bar{T}=\frac{T-T_\infty}{T_W-T_\infty},\bar{C}=\frac{C-C_\infty}{C_W-C_\infty}$$

Non dimensional form of the above equations:

$$\frac{\partial U}{\partial X}+\frac{\partial V}{\partial Y}=0 \quad (5)$$

$$\frac{\partial U}{\partial T}+U\frac{\partial U}{\partial X}+V\frac{\partial U}{\partial Y}=\frac{\partial^2 U}{\partial Y^2}+Gr\bar{T}+Nb\left(\frac{\partial\bar{T}}{\partial Y}.\frac{\partial C}{\partial Y}\right)+Nt\left(\frac{\partial\bar{T}}{\partial Y}\right)^2 \quad (6)$$

$$\frac{\partial\bar{C}}{\partial\tau}+U\frac{\partial\bar{C}}{\partial X}+V\frac{\partial\bar{C}}{\partial Y}=\frac{1}{Le}\left[\frac{\partial^2\bar{C}}{\partial Y^2}+\left(\frac{Nt}{Nb}\right)\frac{\partial^2\bar{T}}{\partial Y^2}\right] \quad (7)$$

The Non dimensional boundary conditions:

$$\tau\geq 0,U=0,V=0,\bar{T}=0,\bar{C}=0 \text{ everywhere}$$

$$\tau>0,U=0,V=0,\bar{T}=0,\bar{C}=0\ at\ X=0$$

$$U=1,V=0,\bar{T}=1,\bar{C}=1\ at\ Y=0$$

$$U=0,V=0,\bar{T}=0,\bar{C}=0\ as\ Y\to\infty$$

Where $G_r = \frac{g\beta(T_W - T_\infty)\upsilon}{U_0^2}$ is the Grashof number, $E_c = \frac{U_0^2}{c_P(T_W - T_\infty)}$ is the Eckert number, $L_e = \frac{\upsilon}{D_B}$ is Lewis number, $N_b = \frac{\tau D_B(C_W - C_\infty)}{\upsilon}$ is Brownian parameter, $N_t = \frac{D_T}{T_\infty}\frac{\tau}{\upsilon}(T_W - T_\infty)$ is thermophoresis parameter, $P_r = \frac{K}{\mu C_p}$ is the Prandtl number.

2.1 Numerical methods:

In order to solve the above non similar unsteady coupled nonlinear partial differential equations with the boundary conditions on the basis of finite difference method. For this a rectangular region is chosen. The region is divided into a grid of lines parallel to X and Y axis, where X axis is taken along the plate and the Y axis is normal to the plate.

Here the plate of height $X_{max}(= 100)$ is considered, i.e., X varies from 0 t0 100 and assumed $Y_{max}(= 25)$, Y varies from 0 to 25. In the following figure there are $m(= 125)$ and $n(= 125)$ grid spacing in the X & Ydirection. Consider ΔX & ΔY are constant mesh size along the X and Y direction and n(=125) grid spacing in the X & Ydirection. Consider ΔX & ΔY are constant mesh size along the X and Y direction $\Delta X = 0.8(0 \le X \le 100)$ and $\Delta Y = 0.2(0 \le Y \le 25)$ with the smaller time step $\Delta\tau = 0.001$.

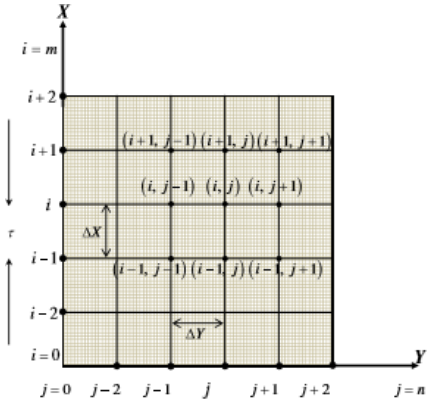

Figure 2: Finite difference method

Let $U', V', \bar{T}', and\ \bar{C}'$ denote the values of $U, V, \bar{T}, \text{and } \bar{T}$ at the end of a time step respectively. Using the explicite finite difference approximation, the following appropriate sets of finite difference equations are obtained:

$$\frac{U'_{i,j} - U'_{i-1}}{\Delta X} + \frac{V_{i,j} - V_{i,j-1}}{\Delta Y} = 0 \tag{8}$$

$$\frac{U'_{i,j} - U_{i,j}}{\Delta\tau} + U_{i,j}\frac{U_{i,j} - U_{i-1,j}}{\Delta X} + V_{i,j}\frac{U_{i,j+1} - U_{i,j}}{\Delta Y} = \frac{U_{i,j+1} - 2U_{i,j} + U_{i,j-1}}{(\Delta Y)^2} + G_r T' \tag{9}$$

$$\frac{\bar{T}'_{i,j} - \bar{T}_{i,j}}{\Delta\tau} + U_{i,j}\frac{\bar{T}_{i,j} - \bar{T}_{i-1,j}}{\Delta X} + V_{i,j}\frac{\bar{T}_{i,j+1} - \bar{T}_{i,j}}{\Delta Y} = \frac{1}{P_r}\left(\frac{\bar{T}_{i,j+1} - 2\bar{T}_{i,j} + \bar{T}_{i,j-1}}{(\Delta Y)^2}\right) + E_c\left(\frac{U_{i,j+1} - U_{i,j}}{\Delta Y}\right)^2 + N_b\left(\frac{\bar{T}_{i,j+1} - \bar{T}_{i,j}}{\Delta Y}\frac{\bar{C}_{i,j+1} - \bar{C}_{i,j}}{\Delta Y}\right) + N_t\left(\frac{\bar{T}_{i,j+1} - \bar{T}_{i,j}}{\Delta Y}\right)^2 \tag{10}$$

$$\frac{\bar{C}'_{i,j} - \bar{C}_{i,j}}{\Delta\tau} + U_{i,j}\frac{\bar{C}_{i,j} - \bar{C}_{i-1,j}}{\Delta X} + V_{i,j}\frac{\bar{C}_{i,j+1} - \bar{C}_{i,j}}{\Delta Y} = \frac{1}{L_e}\left[\left(\frac{\bar{C}_{i,j+1} - 2\bar{C}_{i,j} + \bar{C}_{i,j-1}}{(\Delta Y)^2}\right) + \frac{N_t}{N_b}\left(\frac{\bar{T}_{i,j+1} - 2\bar{T}_{i,j} + \bar{T}_{i,j-1}}{(\Delta Y)^2}\right)\right] \tag{11}$$

With initial and boundary conditions

$$U^0_{i,j} = 0, V^0_{i,j} = 0, \bar{T}^0_{i,j}, \bar{C}^0_{i,j} = 0$$

$$U_{i,j}^{n} = 0, V_{i,j}^{n} = 0, \bar{T}_{0,j}^{0}, \bar{C}_{0,j}^{n} = 0$$

$$U_{i,j}^{0} = 0, V_{i,j}^{0} = 0, \bar{T}_{i,j}^{0}, \bar{C}_{i,j}^{0} = 0$$

$$U_{i,L}^{n} = 0, V_{i,L}^{n} = 0, \bar{T}_{i,L}^{n}, \bar{C}_{i,L}^{n} = 0, \text{ where } L \to \infty$$

Where the subscripts i and j designate the grid points with X and Ycoordinates, respectively, and the superscript n represents a value of time, $\tau = n.\Delta\tau$, where n=0,1,2,...

2.2 Stability and Convergence analysis

To solve this problem here explicit finite difference method is used, so the analysis will remain incomplete unless the stability and convergence of the finite difference scheme is discussed. For the constant mesh sizes, the stability criteria of the scheme may be established as follows. Equation 8 will be ignored since $\Delta\tau$ does not appear in it. The general terms of the Fourier expansion for $U, \bar{T}$ & $\bar{C}$ at a time arbitrarily called $\tau = 0$ are all $e^{i\alpha X}e^{i\beta Y}$, apart from a constant, where $i = \sqrt{-1}$. At a time τ, these terms become

$$U: \boldsymbol{\psi}(\boldsymbol{\tau})e^{i\alpha X}e^{i\beta Y}$$

$$\bar{T}: \boldsymbol{\psi}(\theta)e^{i\alpha X}e^{i\beta Y}$$

$$\bar{C}: \boldsymbol{\psi}(\varphi)e^{i\alpha X}e^{i\beta Y}$$

And after the time step, these terms will become

$$U: \boldsymbol{\psi}'(\boldsymbol{\tau})e^{i\alpha X}e^{i\beta Y}$$

$$\bar{T}: \boldsymbol{\psi}'(\theta)e^{i\alpha X}e^{i\beta Y}$$

$$\bar{C}: \boldsymbol{\psi}'(\varphi)e^{i\alpha X}e^{i\beta Y}$$

Substituting these into equations 9 to 11, with regard to the coefficients U and V as constants over any one time step, we obtain the following equations upon simplification:

$$\frac{\psi'(\tau)-\psi(\tau)}{\Delta\tau} + U\frac{\psi(\tau)(1-e^{-i\alpha\Delta X})}{\Delta X} + V\frac{\psi(\tau)(e^{i\beta\Delta Y}-1)}{\Delta Y} = \frac{2\psi(\tau)(cos\beta\Delta Y-1)}{(\Delta Y)^2} + G_r\theta'(\tau) \quad (12)$$

$$\frac{\theta'(\tau)-\theta(\tau)}{\Delta\tau} + U\frac{\theta(\tau)(1-e^{-i\alpha\Delta X})}{\Delta X} + V\frac{\theta(\tau)\left(e^{i\beta\Delta Y}-1\right)}{\Delta Y} = \frac{1}{P_r}\frac{2\theta(\tau)(cos\beta\Delta Y-1)}{(\Delta Y)^2}$$

$$+E_cU\psi(\tau)\left\{\frac{\left(e^{i\beta\Delta Y}-1\right)}{\Delta Y}\right\}^2 + N_b\bar{C}\theta(\tau)\left\{\frac{\left(e^{i\beta\Delta Y}-1\right)}{\Delta Y}\right\}^2 + N_t\bar{T}\theta(\tau)\left\{\frac{\left(e^{i\beta\Delta Y}-1\right)}{\Delta Y}\right\}^2 \quad (13)$$

$$\frac{\varphi'(\tau)-\varphi(\tau)}{\Delta\tau} + U\frac{\varphi(\tau)(1-e^{-i\alpha\Delta X})}{\Delta X} + V\frac{\varphi(\tau)\left(e^{i\beta\Delta Y}-1\right)}{\Delta Y}$$
$$= \frac{1}{L_e}\left[\left\{\frac{2\varphi(\tau)(cos\beta\Delta Y-1)}{(\Delta Y)^2}\right\} + \frac{N_t}{N_b}\left\{\frac{2\theta(\tau)(cos\beta\Delta Y-1)}{(\Delta Y)^2}\right\}\right] \quad (14)$$

Equations 12, 13, 14 can be written in the following forms:

$$\psi' = A\psi + G_r\Delta\tau\theta'$$

$$\theta' = B\theta + E\psi$$

$$\varphi' = J\varphi + K\theta$$

Where $A = 1 - U\frac{\Delta\tau}{\Delta X}(1-e^{-i\alpha\Delta X}) - V\frac{\Delta\tau}{\Delta Y}\left(e^{i\beta\Delta Y}-1\right) + \frac{2\Delta\tau}{(\Delta Y)^2}(cos\beta\Delta Y-1)$

B

$$= 1 - U\frac{\Delta\tau}{\Delta X}(1-e^{-i\alpha\Delta X}) - V\frac{\Delta\tau}{\Delta Y}\left(e^{i\beta\Delta Y}-1\right) + \frac{1}{P_r}\frac{2\Delta\tau}{(\Delta Y)^2}(cos\beta\Delta Y-1)$$
$$+ N_b\bar{C}\Delta\tau\left\{\frac{\left(e^{i\beta\Delta Y}-1\right)}{\Delta Y}\right\}^2 + N_t\bar{T}\Delta\tau\left\{\frac{\left(e^{i\beta\Delta Y}-1\right)}{\Delta Y}\right\}^2$$

$$E = E_c U \Delta(\tau) \left\{ \frac{\left(e^{i\beta\Delta Y} - 1\right)}{\Delta Y} \right\}^2$$

$$J = 1 - U\frac{\Delta\tau}{\Delta X}(1 - e^{-i\alpha\Delta X}) - V\frac{\Delta\tau}{\Delta Y}\left(e^{i\beta\Delta Y} - 1\right) + \frac{1}{L_e}\frac{2\Delta\tau}{(\Delta Y)^2}(cos\beta\Delta Y - 1)$$

$$K = \frac{1}{L_e}\frac{N_t}{N_b}\left\{\frac{2\Delta(\tau)(cos\beta\Delta Y - 1)}{(\Delta Y)^2}\right\}$$

Again using this assumption we get,

$\psi' = A\psi + G_r\Delta\tau(B\theta + E\psi = C\psi + D\theta$, where $C = A + EG_r\Delta\tau$ & $D = BG_r\Delta\tau$

Therefore, $\psi' = C\psi + D\theta$

$\theta' = B\theta + E\psi$

$\varphi' = J\varphi + K\theta$

This can be expressed in a matrix notation and these equations are

$$\begin{bmatrix}\psi' \\ \theta' \\ \varphi'\end{bmatrix} = \begin{bmatrix}C & D & 0 \\ 0 & B & 0 \\ 0 & K & J\end{bmatrix}\begin{bmatrix}\psi \\ \theta \\ \varphi\end{bmatrix}$$

That is $\eta' = T\eta$ where $\eta' = \begin{bmatrix}\psi' \\ \theta' \\ \varphi'\end{bmatrix}, T = \begin{bmatrix}C & D & 0 \\ 0 & B & 0 \\ 0 & K & J\end{bmatrix}, \eta = \begin{bmatrix}\psi \\ \theta \\ \varphi\end{bmatrix}$

For obtaining the stability condition, we have to find our eigen values of the amplification matrix T, but this study is very difficult since all the elements of T are different. Hence, the problem requires that the Eckert number is assumed to very small, that is tends to zero, Under this consideration, we have $E = 0$, and the amplification matrix becomes

$$T = \begin{bmatrix}C & D & 0 \\ 0 & B & 0 \\ 0 & K & J\end{bmatrix}$$

After simplification of the matrix, we get the following eigen values:

$$\lambda_1 = C, \lambda_2 = B, \lambda_3 = J$$

For stability, each eigenvalue must not exceed unity in modules.

Hence, the stability condition is $|C| \leq 1, |B| \leq 1, |J| \leq 1$

Now we assume that U is everywhere non-negative and V is everywhere non positive.

Thus, $B = 1 - 2[a + b + 2c(\frac{1}{P_r} + N_b\bar{c} + N_t\bar{T})$, where $A = U\frac{\Delta\tau}{\Delta X}, b = |V|\frac{\Delta\tau}{\Delta Y}$ & $C = \frac{\Delta\tau}{(\Delta Y)^2}$

The coefficients a, b, c are all real and non negative. We can demonstrate that the maximum modules of B occurs when $\Delta X = m\pi$ & $\beta\Delta Y = n\pi$, where m and n are integers; hence, B is real. The value of $|B|$ is real. The value of $|B|$ is greater when both m and n are odd integers.

To satisfy the second condition $|B| \leq 1$, the most negative allowable value is $B = -1$

Therefore the first stability condition is

$$2[a + b + 2c\left(\frac{1}{P_r} + N_b\bar{C} + N_t\bar{T}\right)] \leq 2$$

That is, $U\frac{\Delta\tau}{\Delta X} + |V|\frac{\Delta\tau}{\Delta Y} + \frac{2}{P_r}\frac{\Delta\tau}{(\Delta Y)^2} + 2N_b\bar{C}\frac{\Delta\tau}{(\Delta Y)^2} + 2N_t\bar{T}\frac{\Delta\tau}{(\Delta Y)^2} \leq 1$

The third condition $|J| \leq 1$ requires that

$$U\frac{\Delta\tau}{\Delta X}+|V|\frac{\Delta\tau}{\Delta Y}+\frac{2}{L_e}\frac{\Delta\tau}{(\Delta Y)^2}\leq 1$$

Therefore the stability conditions of the method are

$$U\frac{\Delta\tau}{\Delta X}+|V|\frac{\Delta\tau}{\Delta Y}+\frac{2}{P_r}\frac{\Delta\tau}{(\Delta Y)^2}+2N_b\bar{C}\frac{\Delta\tau}{(\Delta Y)^2}+2N_t\bar{T}\frac{\Delta\tau}{(\Delta Y)^2}\leq 1 \;\&$$

$$U\frac{\Delta\tau}{\Delta X}+|V|\frac{\Delta\tau}{\Delta Y}+\frac{2}{L_e}\frac{\Delta\tau}{(\Delta Y)^2}\leq 1$$

From the initial condition, $U=V=\bar{T}=\bar{C}=0$ at $\tau=0$, the consideration due to stability and convergence analysis is $E_c<<1$ and $P_r\geq 0.37, L_e\geq 0.2$.

3. RESULTS AND DISCUSSIONS

The obtained non dimensional, non-linear, coupled partial differential equations can't be solved analytically. For this reason explicit finite difference technique has been applied to solve those equations numerically. The numerical results have been obtained for $m=125$ and $n=125$.

Since the most important fluids are atmospheric air, salt water and water, the results are limited to $P_r=0.30$ (Prandtl number around $0.16-0.70$ for mixtures of noble gases or noble gases with Hydrogen), $P_r=0.63$(Prandtl number for Oxygen), $P_r=0.71$ (Prandtl number for air at 20°C), $P_r=1.0$ (Prandtl number for salt water at 20°C) and $P_r=1.38$ (Prandtl number for gaseous Ammonia). However the values of another parameters such as Lewis number L_e, Brownian motion parameter N_b, thermophoresis parameter N_t and Grashof number G_r are chosen arbitrarily. The profiles of velocity, temperature and concentration of various parameters have been shown graphically in Figs. 3-20.

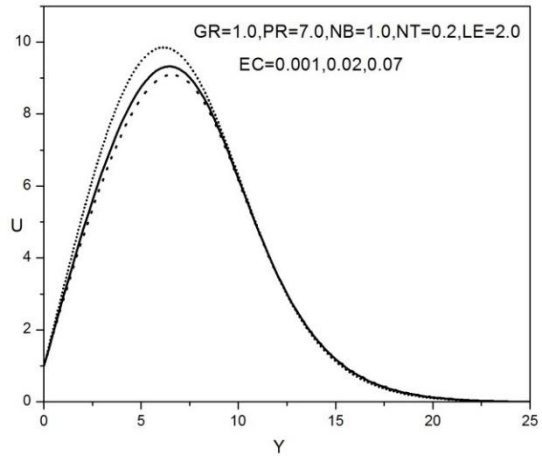

Figure 3: Velocity profiles for different values of Eckert number.

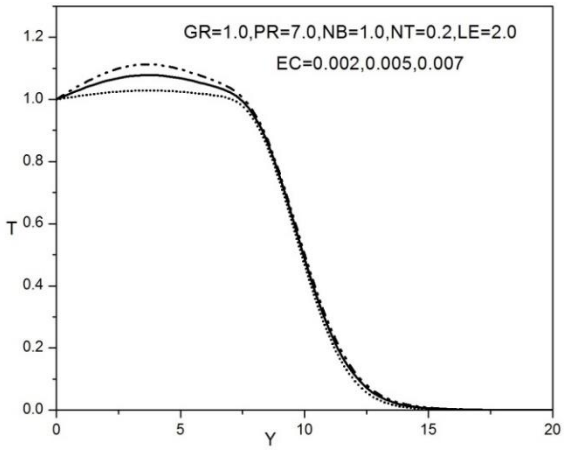

Figure 4: Temperature profiles for different values of Eckert number

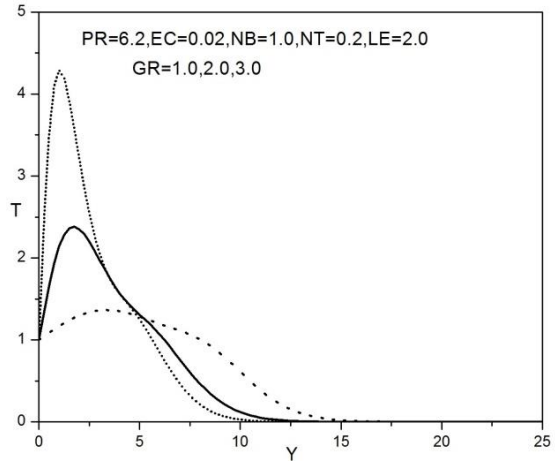

Figure 6: Temperature profiles for different values of Grashof number.

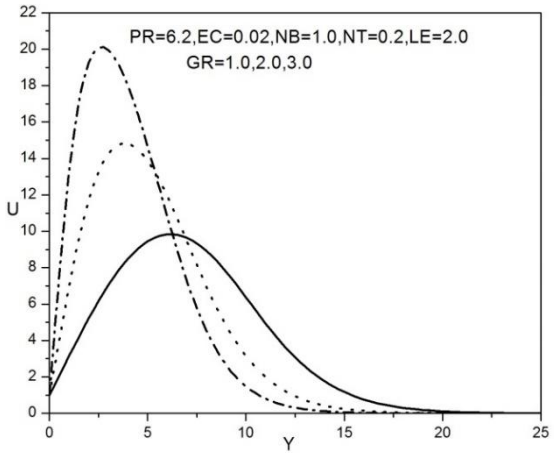

Figure 7: Velocity profiles for different values of Grashof number.

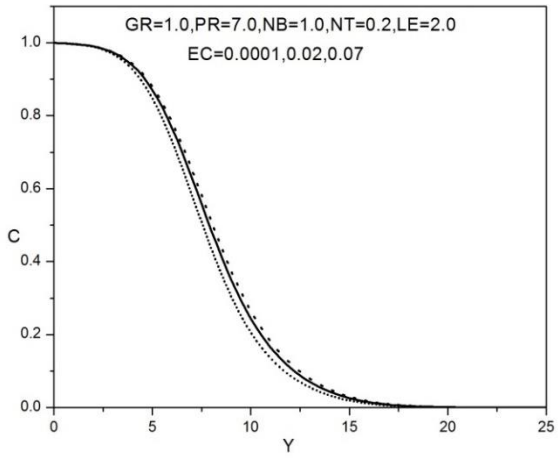

Figure 5: Concentration profiles for different values of Eckert number

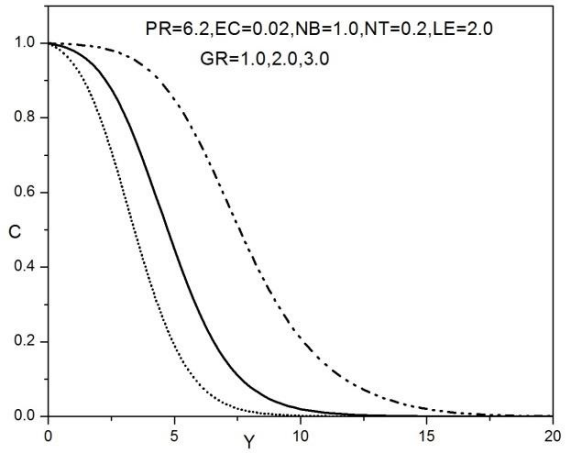

Figure 8: Concentration profiles for different values of Grashof number.

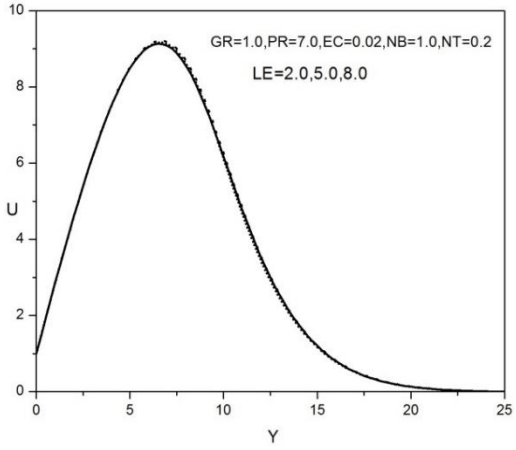

Figure 9: Velocity profiles for different values of Lewis number.

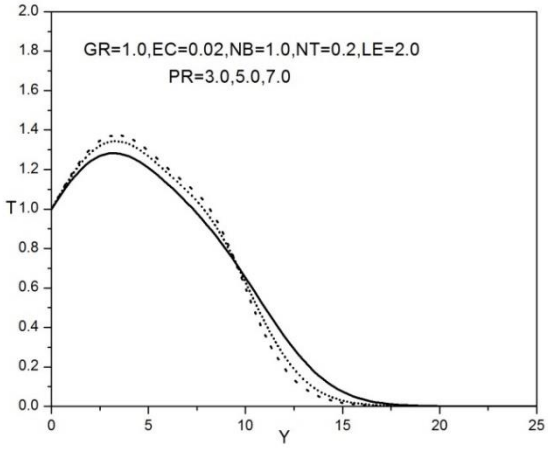

Figure 13: Temperature profiles for different values of Prandtl number.

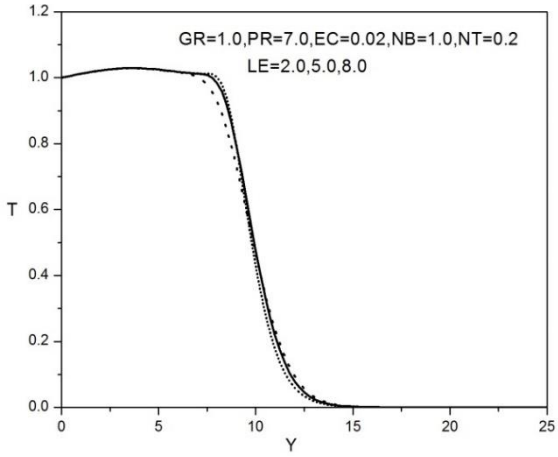

Figure 10: Temperature profiles for different values of Lewis number.

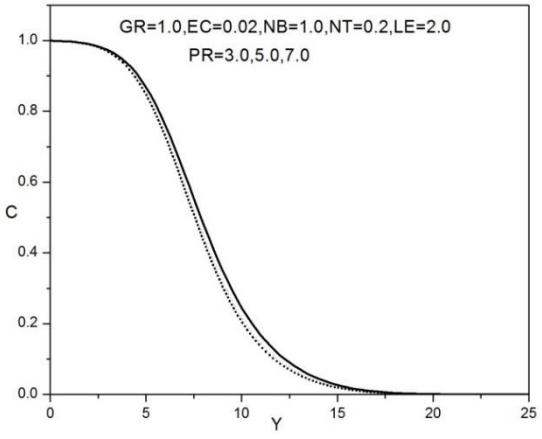

Figure 14: Concentration profiles for different values of Prandtl number.

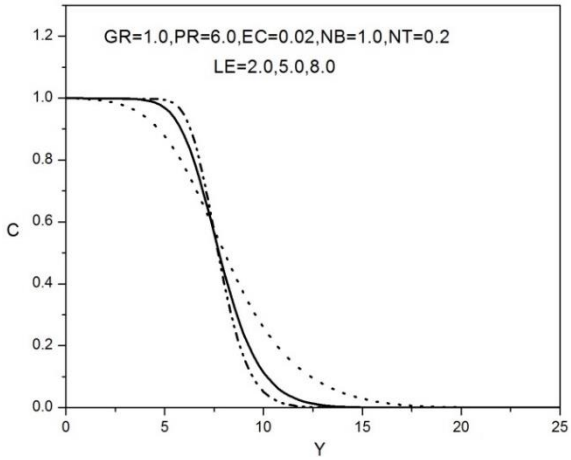

Figure 11: Concentration profiles for different values of Lewis number.

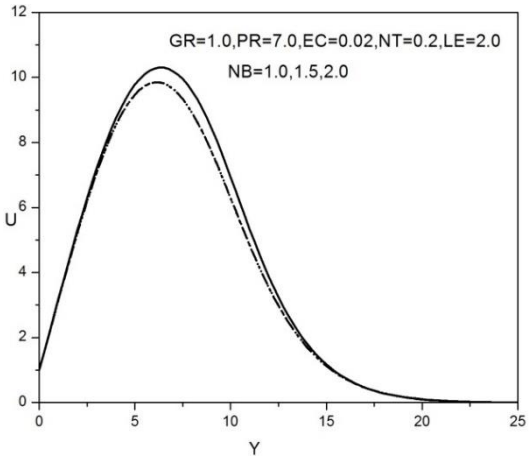

Figure 15: Velocity profiles for different values of Brownin parameter.

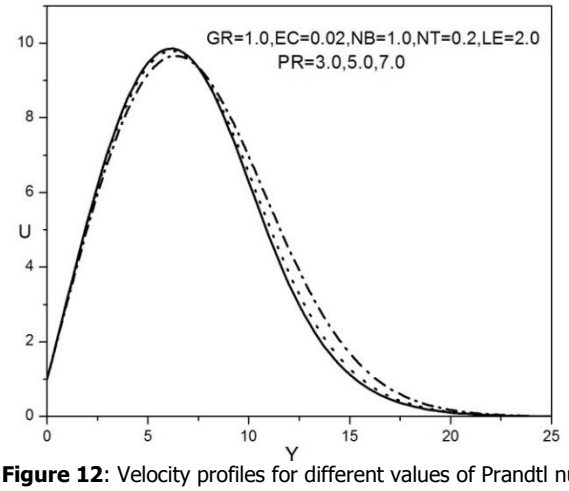

Figure 12: Velocity profiles for different values of Prandtl number.

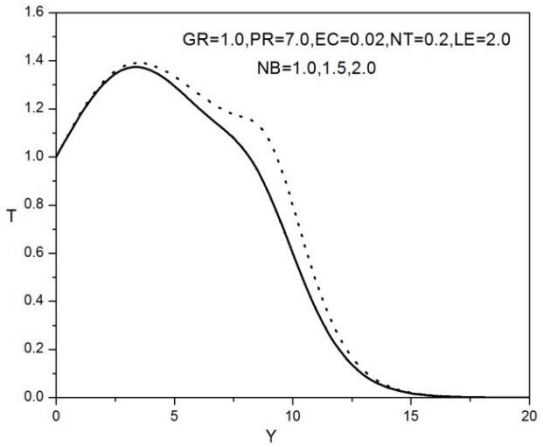

Figure 16: Temperature profiles for the values of Brownin parameter.

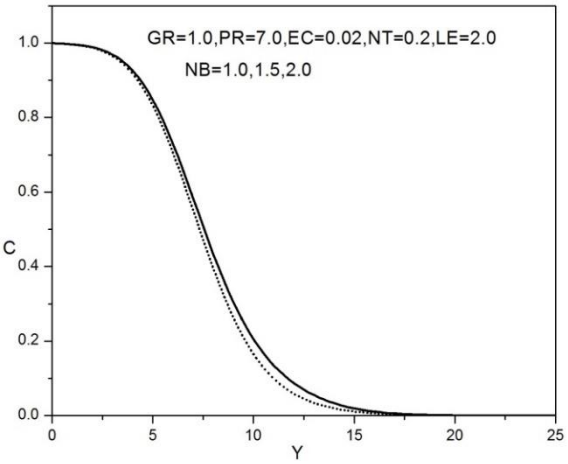

Figure 17: Concentration profiles for different values of Brownian parameter.

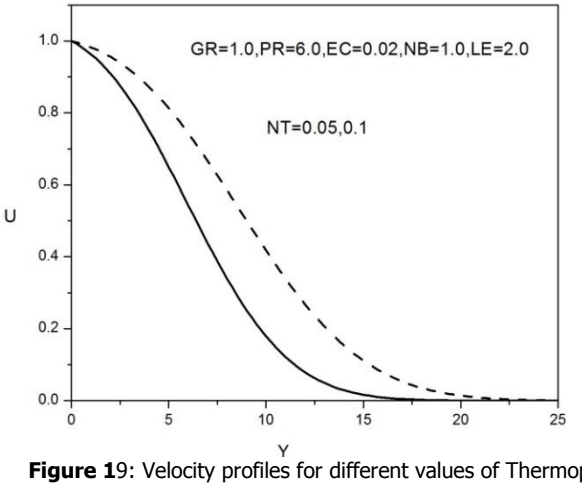

Figure 19: Velocity profiles for different values of Thermophoresis parameter.

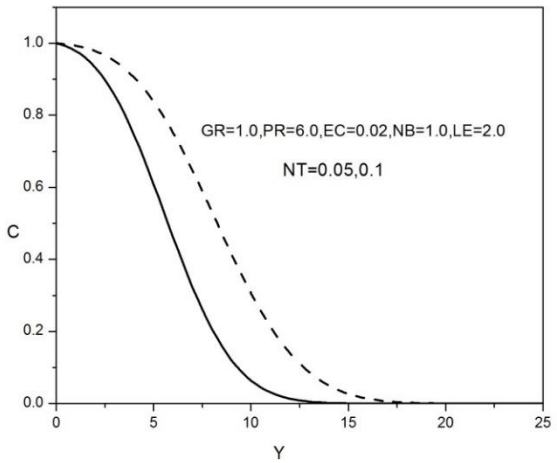

Figure 18: Concentration profiles for different values of Thermophoresis parameter.

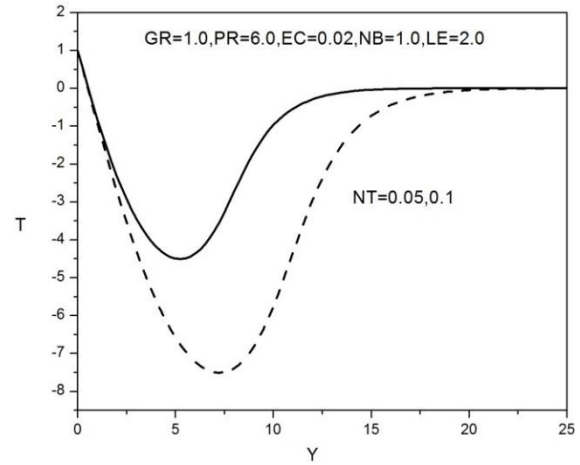

Figure 20: Temperature profiles for different values of Thermophoresis parameter.

The velocity temperature, and concentration profiles for Eckert number have been shown in figure 3, 4, 5 ; for Grashof number have been shown in figure 6, 7, 8, ; for Lewis number have been shown in figure 9, 10, 11; for Prandtl number have been shown in figure 12, 13, 14; for Brownian motion parameter have been shown in figure 15, 16, 17; for thermophoresis parameter have been shown in figure 18, 19, 20.

Here it is observed that when the values of Grashof number G_r increase, then the velocity profiles increase. When the values of Eckert number E_c increase then the temperature profiles also increase, when the values of Prandtl number P_r increase than the temperature profile decrease and when the values of Brownian motion parameter N_b increase than the temperature profile increase. When the values of Thermophoresis parameter N_t increase, then the concentration profile increase, but when the values of Lewis number L_e increase, then the concentration profile decrease.

5. CONCLUSION

Numerical modeling on an unsteady laminar boundary layer flow using Nano fluid with viscous dissipation effect and heat source through a stretching sheet is studied. Using non-dimensional variables the governing equations has been transformed into non-dimensional form and the explicit finite difference method is used with stability and convergence analysis. The non- dimensional time considered here is $\tau = 20$ with $\Delta\tau = 0.0001$. The velocity, temperature and concentration effects on the sheet are studied and shown graphically.
From the present study, the concluding remarks have been taken as follows:

- Larger values of Grashof number showed a significant effect on boundary layer.
- The effect of the Brownian motion and thermophoresis stabilizes the boundary layer growth.
- The boundary layers are highly influenced by the Prandtl number.
- Large Lewis number decreases the concentration profile in the boundary layer.
- The Eckert number has a significant effect on the boundary layer growth.

6. REFERENCES

1. Sakiadis J., Mishra S. R., and. Dash G. C. Chemical reaction effect on MHD Jeffery fluid flow over a stretching sheet through porous media with heat generation/absorption. *International Journal of Applied and Computational Mathematics*. 2017; 3(2): 1225–1238.
2. Crane. L.J.: Flow past a stretching plate. ZAMP. 1970; 21, 645-647.
3. Gorla, R.S.R., Tornabene, R.: Free convection from a vertical plate with non-uniform surface heat flux and embedded in a porous medium. Transp. Porous Media J. 3, 95-106 (1988)
4. Gorla, R.S.R., Zinolabedini, A.: Free convection from a vertical plate with non- uniform surface temperature and embedded in a porous medium. Trans. ASME, J. *Energy Resour. Technol.* 1987; 109, 26-30/
5. Cheng. P., Minkowycz, W.J. Free convection about a vertical flat plate embedded in a saturated porous medium wit applications to heat transfer from a dike. *J. Geophysics Res*. 1977; 82, 2040- 2044.
6. Vajravelu, K., Hadjinicalaou. A.: Heat transfer in a viscous fluid over a stretching sheet with viscous dissipation and internal heat generation. Int. Comm. Heat Mass Trans. 1993; 20: 417-430.
7. Takhar, H.S., Gorla, R.S.R., Soundelgelkar, V.M.: Non-linear one-step method for initial value problems. Int. Num. Meth. Heat Fluid Flow 6, 22-83 (1996)
8. Ghaly, A.Y.: Radiation effect on a certain MHD free convection flow. *Chasos, Solitons Fractal. 2002;* 13, 1843-1850.
9. Rapits. A., Massalas, C.V.: Magnetohydrodynamic flow past a plate by the presence of radiation. *Heat and Mass Transf*. 1998; 34. 107-109.
10. El-Aziz, M.A.: Radiation effect on the flow and heat transfer over an unsteady stretching surface Int. Commu. *Heat and Mass Transf*. 2009; 36, 521-524.
11. Sattar, M.A., Alam, M.M.: Thermal diffusion as well as transpiration effects on M40 free convection and mass transfer flow past an accelerated vertical porous plate. *Indian J. of Pure App. Math*. 1994; 25, 679-688.
12. Na, T.Y., Pop, I.: Unsteady flow past a stretching sheet Mech. *Res Comm*. 1996; 23. 413-422.
13. Singh, P., Jangid, A., Tomer, N.S., Sinha, D. Effects of thermal radiation and magnetic field on unsteady stretching permeable sheet in presence of free stream velocity. *Int. J. Info. And Math*. Sci. 2010; 6(3).
14. Kim, J., Kang, Y.T., Choi, C.K.: Analysis of convective instability and heat transfer characteristics of Nano fluid Phys. *Fluid*s. 2004; 16. 2395-2401.
15. Jang, S.P., Choi, S.U.S.: Effects of various parameters on Nanofluid thermal conductivity. *J. of Heat Transit. 2007;* 129. 617-623
16. Kuznetsov, A.V., Nield, D.A.: The Cheng-Minkowycz problem for natural convective boundary-layer flow in a porous medium saturated by a nanofluid. *Int. J. of Heat and Mass Transf*. 2009; 52: 5792-5795.
17. Kuznetsov, A.V., Nield, D.A.: Natura convective boundary-layer flow of a nanofluid past a vertical plate. *Int. J. of Thermal Sci*. 2010; 49, 243-247.
18. Bachok, N., Ishak, A., Pop, I.: Boundary-layer flow of nanofluids over a moving surface in allowing fluid. *Int. J. of Thermal Sci*. 2010; 49, 1663-1668.
19. Khan, W.A., Pop, I.: Boundary-layer flow of a nanofluid past a stretching sheet. *Int. J. of Heat and Mass Tra*ns. 2010; 53: 2477-2483.
20. Khan, W.A., Pop, I.: Free convection boundary layer flow past a horizontal flat plate embedded in a porous medium field with a nanofluid. *J. Heat Trans.* 2011; 133. 9.
21. Hamad, M.A.A., Pop, I. Scaling transformations for boundary layer stagnation-palm (low towards a heated permeable stretching sheet in a porous medium saturated with a nanofluid and heat absorption/generation effects Transport in Porous Media. 2011; 87: 25-39.
22. Hamad, M.A.A., Pop, I., Ismail, A.I. Magnetic held effects on free convection flow of a nanofluid past a semi-infinite vertical flat pate. *Nonlin. Anal; Real World Appl*. 2011 ;12. 1338-1346.
23. N. Sandeep, V. Sugunamma, and P. Mohan Krishna. Effects of radiation on an unsteady natural convective flow of a EG-Nimonic 80a nanofluid past an infinite vertical plat. *Advances in Physics Theories and Applications*. 2013; 23, 36–43.
24. J. V. Reddy, V. Sugunamma, N. Sandeep, and C. Sulochana. Influence of chemical reaction, radiation and rotation on MHD nanofluid flow past a permeable flat plate in porous medium. *Journal of the Nigerian Mathematical Society*. 2016; 35: 48–65.
25. M. Bilal, S. Hussain, and M. Sagheer. Boundary layer flow of magneto-micropolar nanofluid flow with Hall and ion-slip effects using variable thermal diffusivity. *Bulletin of the Polish Academy of Sciences: Technical Sciences. 2017;* 65(2), 383–390.

Cite this article: Shahmin Suma, M Enamul Karim and Noor Alam. NUMERICAL MODELING ON AN UNSTEADY LAMINAR BOUNDARY LAYER FLOW USING NANO FLUID WITH VISCOUS DISSIPATION EFFECT AND HEAT SOURCE THROUGH A STRETCHING SHEET. *Am. J. innov. res. appl. sci.* 2020; 11(4): 73-82.

This is an Open Access article distributed in accordance with the Creative Commons Attribution Non Commercial (CC BY-NC 4.0) license, which permits others to distribute, remix, adapt, build upon this work non-commercially, and license their derivative works on different terms, provided the original work is properly cited and the use is non-commercial. See: http://creativecommons.org/licenses/by-nc/4.0/